

Pseudopeptide Foldamers – The Homo-Oligomers of Benzyl (4*S*,5*R*)-5-Methyl-2-oxo-1,3-oxazolidine-4-carboxylate

Claudia Tomasini,^[a] Valerio Trigari,^[a] Simone Lucarini,^[a] Fernando Bernardi,^[a] Marco Garavelli,^{*[a]} Cristina Peggion,^[b] Fernando Formaggio,^[b] and Claudio Toniolo^{*[b]}

Keywords: Conformation analysis / Density functional calculations / Foldamers / NMR spectroscopy / Oxazolidin-2-ones

A 2-oxo-1,3-oxazolidine-4-carboxylic acid was designed as a new, conformationally restricted building block for the construction of pseudopeptide foldamers. IR, ¹H NMR and CD techniques, implemented by detailed DFT computational modeling, were exploited to investigate the preferred three-dimensional structure of benzyl (4*S*,5*R*)-5-methyl-2-oxo-1,3-oxazolidine-4-carboxylate homo-oligomers synthesized to the pentamer level. The resulting poly(L-Pro)_n II like helical

conformation was found to be stabilized by intramolecular α-C–H...O=C hydrogen bonds. This novel, acylurethane-based, ternary foldameric structure, if appropriately functionalized, holds promise as a robust template for a variety of applications.

(© Wiley-VCH Verlag GmbH & Co. KGaA, 69451 Weinheim, Germany, 2003)

Introduction

Molecules of a class of unnatural, synthetic oligomers have been recently defined as foldamers by Gellman.^[1] The essential requirement for an oligomer to be included in the foldamer family is to possess a well-defined, repetitive secondary structure, imparted by conformational restrictions of the monomeric unit. In this area of research we described a general method for the synthesis of 2-oxo-oxazolidine-4-carboxylates.^[2] These compounds contain a cyclic urethane moiety, so that by coupling it with a carboxylic acid derivative an imido-type (acylurethane) function is obtained. This latter group is characterized by a nitrogen atom connected to an endocyclic and an exocyclic carbonyl group which tend to adopt a *trans* disposition.^[3] As a consequence of this local rigidity, these oligomers will presumably be forced to fold in an ordered conformation. As an initial step to test this hypothesis, we have recently reported the synthesis of very short homo-oligomers of benzyl (4*S*,5*R*)-5-methyl-2-oxo-1,3-oxazolidine-4-carboxylate (L-Oxd) (Figure 1).^[4]

Here we present the synthesis of an expanded set of these pseudopeptide homo-oligomers (to the pentamer level) complemented by an extended DFT computational investigation and a solution conformational analysis. We have ex-

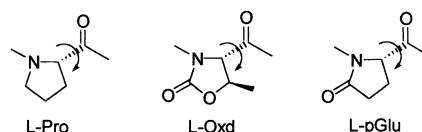


Figure 1. Chemical formula of L-Pro, L-Oxd, and L-pGlu; the rotatable bond is highlighted in each formula

perimentally demonstrated below that these oligo(acylurethanes) are real foldamers with a remarkable conformational preference for a poly(L-Pro)_n II type helix^[5] and that this 3D disposition can be predicted by computational analysis.

Results and Discussion

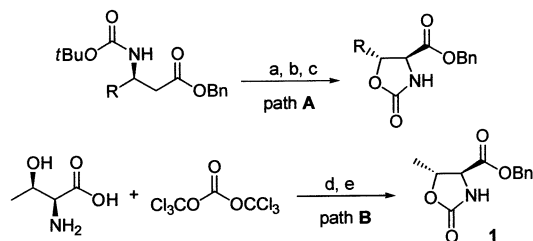
Synthesis and Characterization

Oxazolidin-2-ones are common heterocycles, which can be easily obtained by reaction of vicinal amino alcohols with a synthetic equivalent of carbon dioxide such as phosgene.^[6] These molecules can be cleaved both under strong acidic and under strong basic conditions, but are stable enough to be handled under mild conditions. Enantiomerically pure 4-substituted or 4,5-disubstituted oxazolidin-2-ones have been extensively used as chiral auxiliaries^[7] for a wide range of reactions. Indeed, after acylation of the nitrogen atom, the side chain can be functionalized under a variety of conditions in order to create new stereogenic centers with high stereoselectivity; e.g. alkylations,^[8] and aldol^[9] and pericyclic reactions^[10] have been successfully studied.

^[a] Department of Chemistry “G. Ciamician”, Alma Mater Studiorum, University of Bologna, 40126 Bologna, Italy
Fax: (internat.) + 39-051/209-9456
E-mail: mgara@ciam.unibo.it

^[b] Institute of Biomolecular Chemistry, C.N.R., Department of Organic Chemistry, University of Padova, 35131 Padova, Italy
Fax: (internat.) + 39-049/827-5239
E-mail: claudio.toniolo@unipd.it

The preparation of benzyl (4*S*,5*R*)-5-methyl-2-oxo-1,3-oxazolidine-4-carboxylate (H-L-Oxd-OBn) (**1**) (Scheme 1) can be performed through two different ways: path **A** represents a general synthetic method that allows one to obtain any 5-substituted benzyl (4*S*,5*R*)-2-oxo-1,3-oxazolidine-4-carboxylate from an enantiomerically pure β -amino acid,^[2] while path **B** is a straightforward method from L-threonine,^[11] which allows one to synthesize efficiently only the 5-substituted oxazolidin-2-ones which can be obtained from commercially available amino acids. In this work we have exploited the latter method to synthesize **1** on a multigram scale.

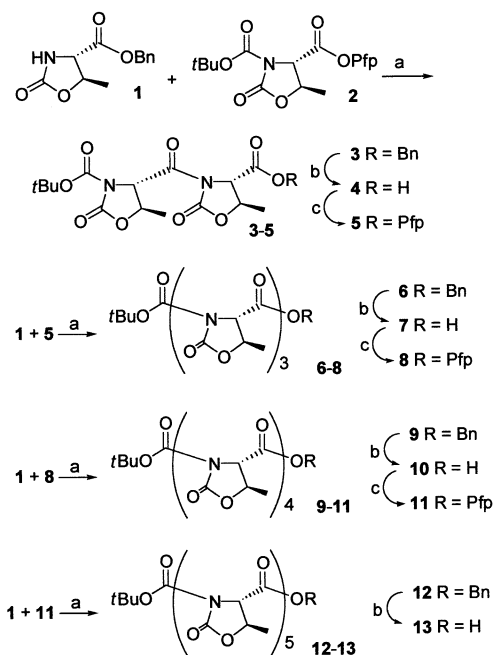


Scheme 1. Synthetic routes for H-L-Oxd-OBn (**1**); reagents and conditions: (a) LiHMDS (2 equiv.), dry THF ($-60\text{ }^{\circ}\text{C}$); (b) I_2 (1.2 equiv.), dry THF, ($-60\text{ }^{\circ}\text{C}$); (c) $\text{Sn}(\text{OTf})_2$, dry CH_2Cl_2 ; (d) 1 N NaOH, DMF; (e) BnBr (1.1 equiv.), TEA, acetone

The acylation step is not straightforward. It was originally achieved by formation of the lithium salt of the oxazolidin-2-one with *n*-butyllithium, followed by addition of the acid chloride.^[12] Recently, a different procedure was envisaged to eliminate the use of *n*-butyllithium; the oxazolidin-2-one may be efficiently acylated with a mixed anhydride using triethylamine and a slight molar excess of lithium chloride.^[13] In our case we had to perform a homo-oligomerization, so that the acylation source was the 2-oxo-oxazolidine-4-carboxylate itself. As the corresponding acyl chloride is unstable, Boc-L-Oxd-OBn (Boc: *tert*-butoxy-carbonyl) was transformed into the corresponding pentafluorophenyl ester Boc-L-Oxd-OPfp (**2**) under mild conditions.^[14] The coupling reaction was performed by treating H-L-Oxd-OBn (**1**) with **2** in the presence of diisopropylethylamine (DIEA) and 4-(dimethylamino)pyridine (DMAP) (Scheme 2). According to the same procedure, homo-oligomers up to the pentamer level were synthesized.

DFT Computational Modeling

Molecular mechanics and molecular dynamics are the conventional tools used for modeling oligomers and for conformational search and analysis. These are very convenient approaches when the size of the molecular system under investigation is progressively increased; however, a heavy dependence of the reliability of the results obtained on the quality of the force field used was often observed. This drawback is particularly crucial in the description of weak hydrogen bonds which can be involved in the stabilization of complex molecular architectures. In a previous work^[15] we showed that weak intramolecular hydrogen bonds (such as $\text{C}-\text{H}\cdots\text{O}=\text{C}$) play an important role in the stabilization



Scheme 2. Synthetic routes for the (L-Oxd)_n homo-oligomers; reagents and conditions: (a) DIEA (4 equiv.), DMAP (0.1 equiv.), dry DMF, room temp., 16 h; (b) H_2 , Pd/C (10%), EtOAc, room temp., 1 h; (c) $\text{CF}_3\text{CO}_2\text{C}_6\text{F}_5$ (1.25 equiv.), pyridine (1.1 equiv.), dry DMF, room temp., 1 h

of conformational minima for the (L-pGlu)_n foldameric structures (Figure 1). Therefore, we carried out our calculations on these systems at a fully correlated level using density functional theory (DFT) with both a well-tested functional and a basis set.

A preliminary ^1H NMR characterization of dimer **3**, trimer **6**, and tetramer **9** of the Boc-(L-Oxd)_n-OBn series, reported by us in a previous paper,^[4] indicated that a homo-oligomer composed by *n* L-Oxd monomers has *n* – 1 downfield shifted α -CH proton signals. These anomalous chemical shift values were tentatively associated with the occurrence of weak $\alpha\text{-C}-\text{H}\cdots\text{O}=\text{C}$ hydrogen bonds.

To determine the conformational minima for the (L-Oxd)_n oligomers and to obtain a more accurate explanation of their magnetic properties, in this work we carried out fully unconstrained DFT optimizations for dimer **3**, trimer **6**, tetramer **9** and pentamer **12**. The starting structures used for DFT optimization and refinement of dimer **3** and trimer **6** were initially located by a preliminary AM1 optimized surface scanning about the relevant free rotatable dihedral angles of the oligomeric skeleton: N1–C1A–C1–N2 for the dimer, and N1–C1A–C1–N2 and N2–C2A–C2–N3 for the trimer. Note that the imide bonds are not free to rotate. Subsequently, the DFT-optimized structures for dimer **3** and trimer **6** were exploited as templates to generate the starting geometries for the DFT optimizations of the longer analogues **9** and **12**.

For dimer **3** the optimized bond lengths and angles between the atoms C1A, H1A, O2D and C2D involved in the hypothetical $\alpha\text{-C}-\text{H}\cdots\text{O}=\text{C}$ interaction have the following

values: the optimized H1A–O2D bond length is 2.34 Å, while the optimized H1A–O2D–C2D bond angle and C1A–H1A–O2D–C2D dihedral angle are 97.7 and 52.0°, respectively. These data are in agreement with those reported in the literature for related systems; in particular, the mean hydrogen bond length for this kind of interaction is 2.4 Å and the bond angle may vary from 90 to 180°.^[16] Therefore, the fully relaxed structure of **3** does seem to involve an α -C–H \cdots O=C interaction (see Figure 2 and the first column of Table 1), as recently shown for the related (L-pGlu)₂ oligomer.^[15] Quite remarkably, this latter structure is almost identical to the one reported here (Figure 2), thus providing an indirect validation of the method employed.

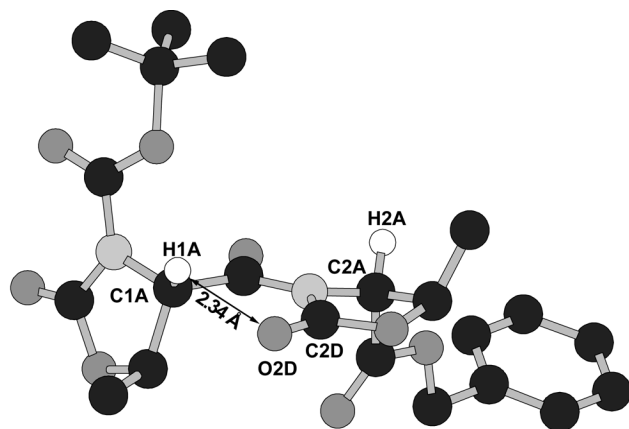


Figure 2. DFT-optimized structures for the dimer **3** with partial atom labeling; for clarity only the H-bonded hydrogen atoms are shown

To further validate the optimized structure for dimer **3**, the ¹H NMR chemical shift (δ) values for its H1A and H2A protons were simulated^[17,18] and compared to those observed in a CDCl₃ solution. These data are reported in the first two columns of Table 2. The experimental results show a chemical shift of $\delta = 4.59$ ppm for proton H2A but also a downfield signal at $\delta = 5.49$ ppm for proton H1A induced by the deshielding effect of the H1A \cdots O2D hydrogen bond. Although consistently shifted to higher field by ca. 0.4 ppm (this effect is due to the approximation of the simulation method used here, as documented elsewhere),^[15,17,18] the simulated chemical shift values for H1A and H2A ($\delta = 4.22$ ppm and $\delta = 5.12$ ppm, respectively) do in fact exhibit the same trend as that of the experimental data. In conclusion, it is now possible to ascribe the anomalous downfield chemical shift computed and observed for the proton H1A in **3** to the noncovalent H1A \cdots O2D interaction. Therefore, we experimentally demonstrated that the presence of a weak hydrogen bond originates a signal for the related proton to lower field by ca. 1 ppm. On the other hand, if this interaction is not taken into account in the computations, this proton signal would be observed in its normal range of chemical shifts. We have previously estimated the strength for such a weak α -CH \cdots O=C interaction to be about 1.5 kcal/mol^{−1}.^[15]

The lowest-energy minimum for trimer **6** was optimized in a similar fashion (Figure 3). According to the procedure outlined above, DFT optimizations for the longer analogues (i.e. the homo-oligomers **9** and **12**) were also performed. In all these cases, after the full relaxation (i.e. an unconstrained optimization), we found that the atoms involved in the hypothetical α -C–H \cdots O=C interactions^[4] possess the

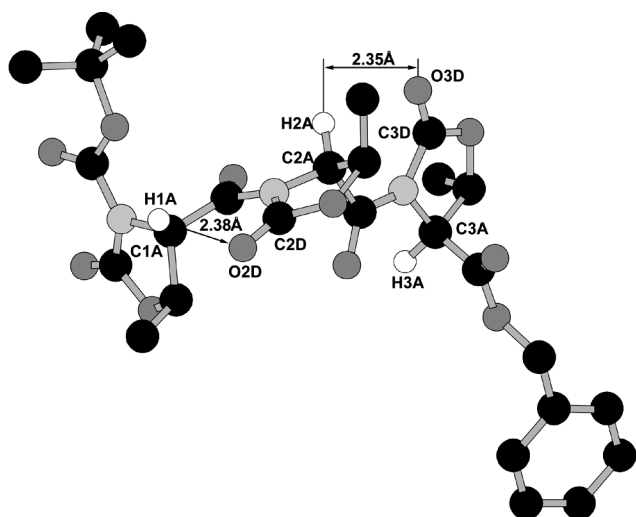
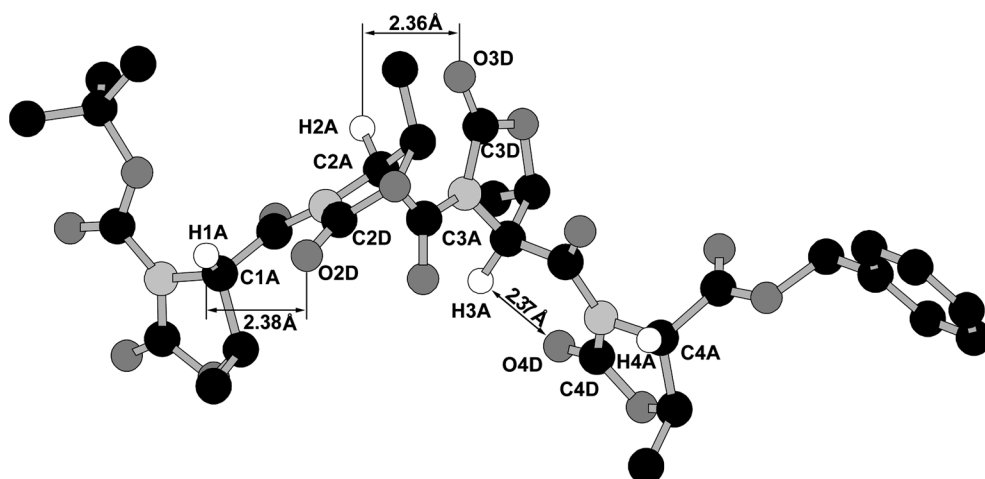
Table 1. Calculated geometrical parameters for dimer **3**, trimer **6**, tetramer **9** and pentamer **12**

Dimer 3	Trimer 6	Tetramer 9	Pentamer (12)
Bond length [Å]	Bond length [Å]	Bond length [Å]	Bond length [Å]
H1A–O2D 2.34	H1A–O2D 2.38 H2A–O3D 2.35	H1A–O2D 2.38 H2A–O3D 2.36 H3A–O4D 2.37	H1A–O2D 2.36 H2A–O3D 2.37 H3A–O4D 2.38 H4A–O5D 2.38
Bond angle [°]	Bond angle [°]	Bond angle [°]	Bond angle [°]
C1A–H1A–O2D 108.7 H1A–O2D–C2D 97.7	C1A–H1A–O2D 106.0 C2A–H2A–O3D 107.1 H1A–O2D–C2D 97.0 H2A–O3D–C3D 96.5	C1A–H1A–O2D 106.1 C2A–H2A–O3D 105.3 C3A–H3A–O4D 105.1 H1A–O2D–C2D 96.5 H2A–O3D–C3D 95.9 H3A–O4D–C4D 96.9	C1A–H1A–O2D 106.9 C2A–H2A–O3D 105.0 C3A–H3A–O4D 103.1 C4A–H4A–O5D 104.3 H1A–O2D–C2D 96.8 H2A–O3D–C3D 96.0 H3A–O4D–C4D 96.3 H4A–O5D–C5D 97.2
Dihedral angle [°]	Dihedral angle [°]	Dihedral angle [°]	Dihedral angle [°]
C1A–H1A–O2D–C2D 52.0	C1A–H1A–O2D–C2D 56.8 C2A–H2A–O3D–C3D 58.1	C1A–H1A–O2D–C2D 57.9 C2A–H2A–O3D–C3D 61.3 C3A–H3A–O4D–C4D 59.0	C1A–H1A–O2D–C2D 56.8 C2A–H2A–O3D–C3D 61.1 C3A–H3A–O4D–C4D 61.5 C4A–H4A–O5D–C5D 57.9

Table 2. Calculated and experimental (CDCl₃ solution) chemical shifts (δ in ppm) for dimer **3**, trimer **6**, tetramer **9** and pentamer **12**

Proton	Dimer 3		Trimer 6		Tetramer 9		Pentamer 12	
	calcd.	exp.	calcd.	exp.	calcd.	exp.	calcd.	exp.
H1A	5.12	5.49	5.02	5.47	4.97	5.46	5.00	5.48
H2A	4.22	4.59	5.32	5.62	5.28	5.63	5.25	5.62
H3A			4.17	4.56	5.29	5.57	5.20	5.58
H4A					4.16	4.54	5.26	5.58
H5A							4.06	4.55

correct geometrical features to allow for the onset of these hydrogen bonds. Remarkably, the average values for the H \cdots O bond length and the H \cdots O=C bond angle are 2.37 Å and 96.7°, respectively (Figures 2–5 and Table 1), being similar to those computed for dimer **3** and with the values reported in the literature for related interactions and similar systems.^[15,16]

Figure 3. DFT-optimized structures for the trimer **6** with partial atom labeling; for clarity only the H-bonded hydrogen atoms are shownFigure 4. DFT-optimized structures for the tetramer **9** with partial atom labeling; for clarity only the H-bonded hydrogen atoms are shown

Moreover, we performed a calculation of chemical shifts^[17,18] for protons H1A, H2A and H3A in trimer **6**, H1A, H2A, H3A and H4A in tetramer **9**, and H1A, H2A, H3A, H4A and H5A in pentamer **12**. As expected, the calculated δ values for the protons involved in the noncovalent α -C–H \cdots O=C interaction are ca. 1 ppm higher than the chemical shifts for the free protons. The simulated values (Table 2) are very close to the experimental data (except for the 0.4 ppm higher field shift consistently seen in the signals) and both sets of values show the same progress (Figure 6). Therefore, we may deduce that for each homo-oligomer there are $n - 1$ (where n is the number of monomers in each molecule) downfield proton signals and, as a consequence, that there are also $n - 1$ α -C–H \cdots O=C hydrogen bonds. These interactions, although weak, do stabilize the overall secondary structure allowing the molecule to adopt a robust poly(L-Pro)_{*n*} II type helix (3₁ helix).^[5] Front and side views of the ternary helix optimized for pentamer **12** are reported in Figure 7 (part a and b, respectively).

Although these computational findings do not provide an ultimate proof for the ordered foldameric structure in the longest homo-oligomers, we still believe that these data, when combined with experimental results, do offer a significant clue for the stability of the afore-mentioned foldamer conformations. In addition, the experimental ¹H NMR analysis, when complemented and supported by computational modeling, does represent a valid tool to elucidate the secondary structure of these molecules.

Solution Conformational Analysis

Information on the preferred conformation of the L-Oxd homo-oligomers in solution was obtained in structure-supporting solvents, CDCl₃ and methanol (MeOH), by FT-IR absorption, ¹H NMR and CD techniques.

Figure 8 illustrates the FT-IR absorption spectra (C=O stretching region) of the Boc/Obn-protected L-Oxd series to the pentamer level. A strictly comparable trend was observed for the C-deprotected series (not shown). From literature data on imides and acylurethanes^[19] and a visual in-

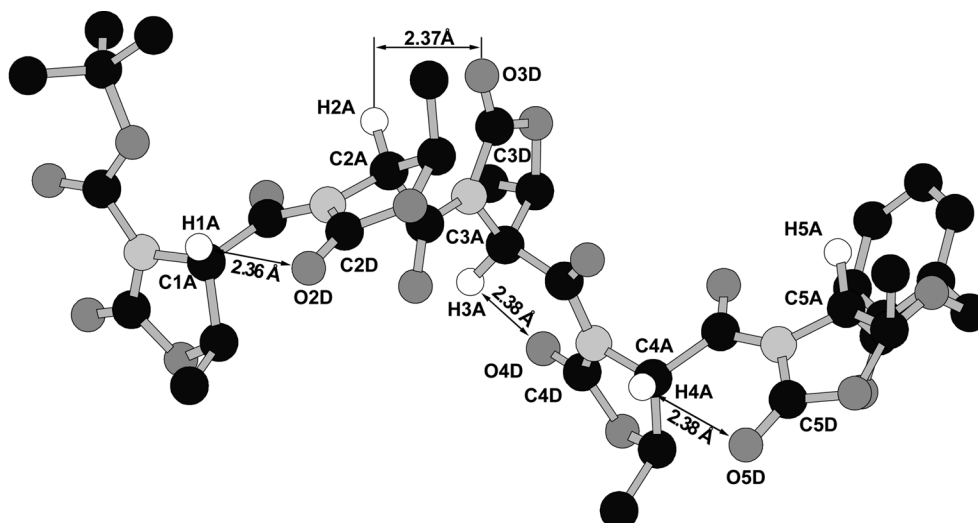


Figure 5. DFT-optimized structures for the pentamer **12** with partial atom labeling; for clarity only the H-bonded hydrogen atoms are shown

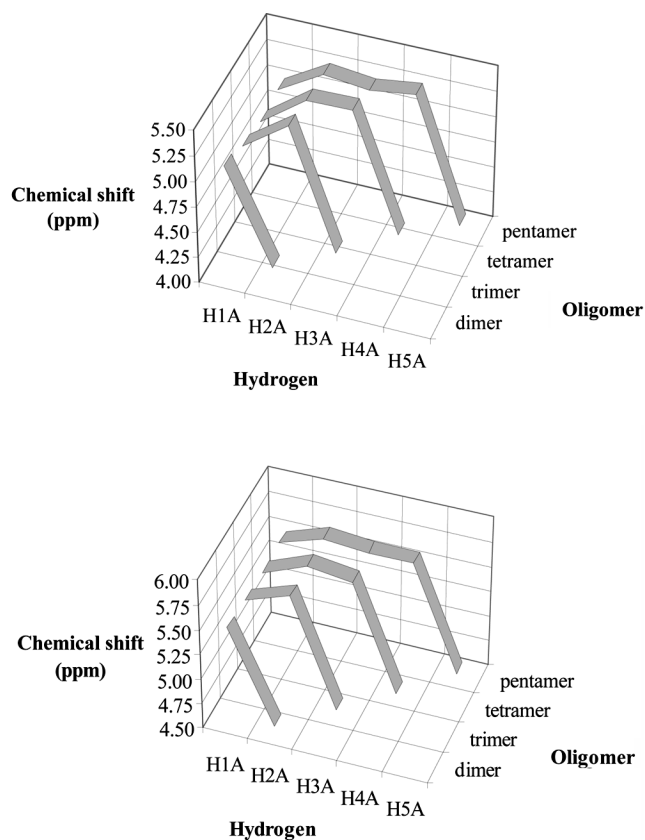


Figure 6. Progress of the calculated (top) and experimental (CDCl_3 solution) (bottom) chemical shifts for the homo-oligomers **3**, **6**, **9** and **12**

spection of the spectra in Figure 8 it is evident that the major contribution to all four bands in the $1830\text{--}1700\text{ cm}^{-1}$ region is given by the carbonyl stretching absorptions of the acylurethane moiety. In particular, the intensity of the two bands near 1790 and 1720 cm^{-1} regularly increases with oligomer backbone lengthening. The contribution to the

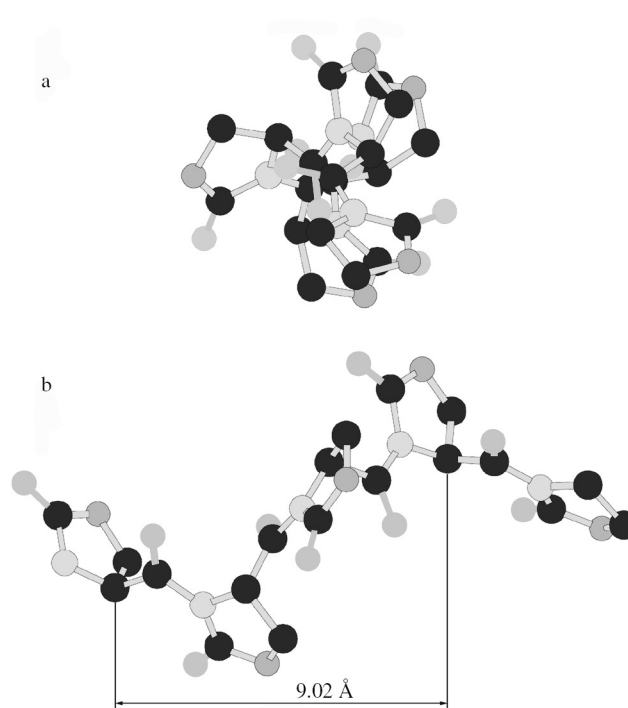


Figure 7. Front view (a) and side view (b) of the calculated pentamer **12** helix; the terminally protecting groups have been removed for clarity

spectra in this region from the COOBn (in the ester series) and COOH (in the free carboxylic acid series) groups is expected to be of minor significance and located near $1740^{[20]}$ and 1710 cm^{-1} ,^[19a] respectively. From this FT-IR absorption analysis it may be concluded that there is no evidence of any abrupt conformational change in a CDCl_3 solution as the pseudopeptide main chain elongates.

In this Boc/OBn-protected L-Oxd series the only potentially informative protons for a ^1H NMR conformational analysis are the $\alpha\text{-CH}$ protons. To obtain additional, more

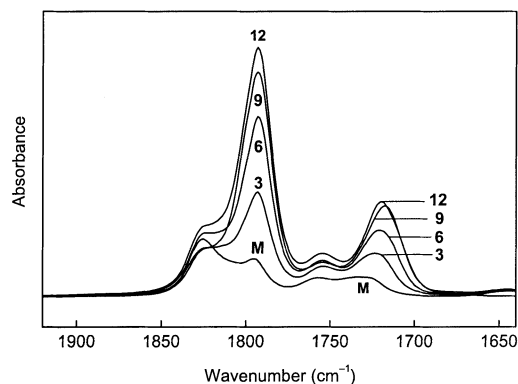


Figure 8. FT-IR absorption spectra in the 1900–1650 cm^{-1} region of the monomer Boc-L-Oxd-OBn (**M**) and the higher homo-oligomers **3**, **6**, **9**, and **12** in a CDCl_3 solution; peptide concentration 1 mM

detailed information on the preferred conformation in a CDCl_3 solution of Boc-(L-Oxd)₅-OBn (**12**), the longest and most significant homo-oligomer of this series, we carried out a 400-MHz ^1H NMR investigation by use of the DMSO dependence of an α -CH proton chemical shift. This solvent has a strong hydrogen-bonding acceptor character and, if bound to an acidic proton, is expected to dramatically move its chemical shift downfield.^[21]

As discussed above, from Figure 9 it is evident that in a CDCl_3 solution the chemical shifts of all α -CH protons, except that assigned to the C-terminal residue (H5A), cluster in a region largely downfield compared to that common to peptide α -CH protons ($\delta \approx 4.5$ –5.0 ppm)^[22] and especially to the α -CH protons of poly(L-Pro)_n II ($\delta = 4.80$ ppm).^[23] We ascribed this unusual shift to the presence of a 2-oxo-1,3-oxazolidine carbonyl group in the vicinity of the N-terminal and internal α -CH protons. This α -C–H \cdots O=C interaction is clearly absent in the case of the C-terminal α -CH proton, that therefore resonates in the expected spectral region. In our ^1H NMR titration experiments two classes of α -CH protons were observed: (1) The first class (H1A–H4A protons) includes protons whose chemical shifts are insensitive to the addition of the perturbing agent DMSO. (2) The second class (H5A proton) includes that displaying a behaviour characteristic of at least partially exposed protons (moderate sensitivity of chemical shift to solvent composition). The present ^1H NMR spectroscopic data support the view that in a solvent of low polarity (CDCl_3) the H1A–H4A protons of the pentamer are inaccessible to the perturbing agent and therefore, most probably, are intramolecularly hydrogen-bonded.

The electronic absorption spectra of the acylurethane chromophore of the Boc-protected L-Oxd homo-oligomers in an MeOH solution are characterized by a moderately intense ($\epsilon_R = 2000$ –2500) transition in the 200–250 nm region centred at ca. 210 nm (not shown). The related chiroptical properties are illustrated in Figure 10. While the monomer exhibits a single, weak and positive band (at ca. 215 nm) at > 200 nm, the CD spectra of the higher oligomers show dichroic doublets of regularly increasing in-

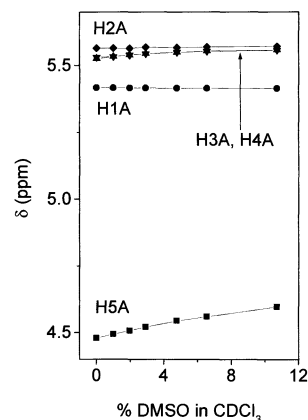


Figure 9. Plot of α -CH chemical shifts in the ^1H NMR spectra of the homo-pentamer Boc-(L-Oxd)₅-OBn (**12**) as a function of increasing percentages of DMSO to the CDCl_3 solution (v/v); peptide concentration 1 mM

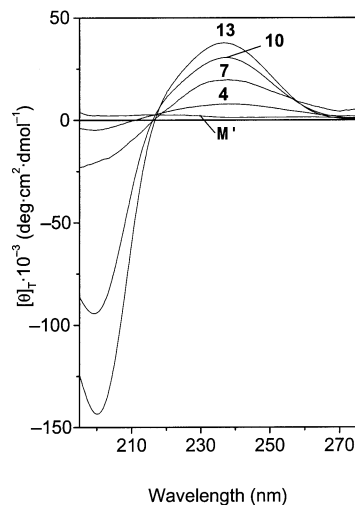


Figure 10. CD spectra in the 195–270 nm region of the monomer Boc-L-Oxd-OH (**M'**) and the higher homo-oligomers **4**, **7**, **10**, and **13** in an MeOH solution; peptide concentration 1 mM

tensity with increasing backbone length. In these spectra the positive lobe is lower in intensity than the negative lobe and the crossover point is at 212–216 nm. Also, these curves give rise to a nearly isodichroic point in the vicinity of 217 nm. The CD spectra of the benzyl ester oligomers (not shown) strictly compare with those reported in Figure 10. As there is no published systematic investigation of the complex semicyclic acylurethane nor of the related imide chromophore,^[24] and in view of the lack of a precise correlation of the positions of the UV absorption bands versus the wavelengths of the positive/negative maxima and cross-over points in the CD spectra of our homo-oligomers, we made no attempt to assign the observed Cotton effects to any specific electronic transition. However, the shape similarity and the regularly increasing intensity of the CD spectra with main-chain elongation to the pentamer point to the persistence of the same backbone conformation for these L-Oxd oligomers in an MeOH solution. We also

checked the conformational stability of a representative homo-oligomer, the tetramer, by recording the CD spectra in an MeOH solution as a function of heating from 20 to 50 °C (not shown). In this temperature range the conformation appears to be remarkably stable as no change in the shape and only a modest decrease (less than 10%) in the band intensities were observed.

Conclusions

When joined in specific sequences, physicochemical information inherent in the α -amino acid monomeric units enables the onset of functional folded peptide and protein architectures. This property of biopolymers can provide a valuable basis to our attempts to design novel materials aimed at emulating catalytic processes, energy and electron transfer mechanisms, and self-organizing phenomena.

In this work we designed, synthesized and determined^[25] the conformational preference of a novel pseudopeptide foldameric series based on L-Oxd building blocks characterized by a semi-extended helical conformation. As in the related poly(L-Pro)_n II^[5] and (L-pGlu)_n^[15] (Figure 1) helices, the torsion angle is frozen in a *skew* conformation (from –50 to –80°) by virtue of the steric restriction imposed by the five-membered ring system, while the ψ and ω torsion angles are close to *trans* (from 140 to 160°) and *trans* (180°), respectively. All three are left-handed, elongated, ternary helices with an α -C¹... α -C⁴ distance (pitch) of 9.0–9.5 Å. Obviously, the stabilizing α -C–H...O=C intramolecular hydrogen bond characteristic of the (L-Oxd)_n and (L-pGlu)_n helices is absent in the poly(L-Pro) II helix. It may be anticipated that, for this reason and for the stable *anti* disposition of the two carbonyl groups of each semicyclic acylurethane or imide system, the (L-Oxd)_n and (L-pGlu)_n polymers are not expected to exhibit the amide *cis-trans* dynamic equilibrium typical of the related poly(L-Pro)_n I \rightleftharpoons II helices.^[5]

As this phenomenon, particularly significant in short homo-oligomers,^[26] is responsible for the onset of multiple coexisting conformers, it is evident that the (L-Pro)_n oligopeptides, unless ω -frozen by a bulky substitution in position 5 of the pyrrolidine ring,^[27,28] cannot be safely exploited as molecular rulers with well-predetermined distances. On the other hand, the rigid (L-Oxd)_n homo-oligomeric system, as its γ -lactam (L-pGlu)_n counterpart, if adequately functionalized in position 5, is expected to be a very useful scaffold in future investigations relating chemistry to biology and material sciences. In this connection it is worth mentioning that a qualitative check on the (L-Oxd)_n homo-oligomers points to a definite, although moderate, water solubility.

Although neither of these findings does provide per se an ultimate proof for the geometry of the most stable structure of the (L-Oxd)_n homo-oligomers, still all these data, when taken in conjunction with our recent results on the related (L-pGlu)_n system,^[15] provide a satisfactory interpretation of this unique type of foldameric structure.

Experimental Section

Synthesis and Characterization: Materials and reagents were of the highest commercially available grade and used without further purification. Reactions were monitored by thin-layer chromatography using Merck silica gel 60 F254 covered plastic plates. Compounds were visualized by UV light and ceric ammonium molybdate. Flash chromatography was performed using a Merck silica gel 60 stationary phase. ¹H and ¹³C NMR spectra were recorded with a Varian Gemini 300 or a Varian Mercury 400 spectrometer. Chemical shifts are reported in δ values relative to the solvent peak of CHCl₃, set at δ = 7.27 ppm. Infrared spectra were recorded with a Nicolet 210 FT-IR absorption spectrometer. Melting points were determined in open capillaries and are uncorrected.

Benzyl (4*S*,5*R*)-5-methyl-2-oxo-1,3-oxazolidine-4-carboxylate (1, Scheme 1): This oxazolidin-2-one, starting material for the synthesis of the homo-oligomers, was obtained by reaction of L-threonine with triphosgene, according to the method described by Hassner and co-workers.^[11]

General Procedure for the Synthesis of the Homo-Oligomers of Benzyl (4*S*,5*R*)-5-Methyl-2-oxo-1,3-oxazolidine-4-carboxylate (Scheme 2): The detailed procedures for the steps of protection, deprotection, activation and coupling, along with the characterization data for Boc-L-Oxd-OBn (1), and compounds 2, 3, 6, 7, 8 and 9, are also reported in ref.^[4]

Boc-(L-Oxd)₃-OH (4): Yield: 95% (0.95 mmol, 0.47 g); m.p. 132 °C. $[\alpha]_D^{20}$ = –142.5 (*c* = 1.0, CH₂Cl₂). ¹H NMR (400 MHz, CDCl₃): δ = 1.50 (s, 9 H, *t*Bu), 1.52–1.75 (m, 9 H, 3 Me), 4.56 (d, ³*J*_{H,H} = 3.2 Hz, 1 H, CHN), 4.70 (dq, ³*J*_{H,H} = 1.0, 6.6 Hz, 1 H, CHO), 4.75–4.91 (m, 2 H, 2 CHO), 5.49 (d, ³*J*_{H,H} = 1.0 Hz, 1 H, CHN), 5.65 (d, ³*J*_{H,H} = 1.0 Hz, 1 H, CHN), 6.61 (br. s, 1 H, OH) ppm. ¹³C NMR (100 MHz, CDCl₃): δ = 20.6, 21.2, 27.8, 60.7, 61.1, 62.0, 65.9, 73.1, 75.5, 85.0, 149.0, 151.5, 152.0, 152.3, 166.6, 168.3, 169.0 ppm. IR (Nujol): $\tilde{\nu}$ = 1791, 1718 cm^{–1} (C=O). C₂₀H₂₅N₃O₁₂ (499.14): calcd. C 48.10, H 5.05, N 8.41; found C 48.06, H 5.09, N 8.44.

Boc-(L-Oxd)₃-OPfp (5): Yield: 90% (0.90 mmol, 0.60 g). ¹H NMR (300 MHz, CDCl₃): δ = 1.53 (s, 9 H, *t*Bu), 1.64 (d, ³*J*_{H,H} = 6.3 Hz, 3 H, Me), 1.69 (d, ³*J*_{H,H} = 6.3 Hz, 3 H, Me), 1.76 (d, ³*J*_{H,H} = 6.0 Hz, 3 H, Me), 4.70 (dq, ³*J*_{H,H} = 1.8, 6.3 Hz, 1 H, CHO), 4.76 (dq, ³*J*_{H,H} = 2.1, 6.3 Hz, 1 H, CHO), 4.88–5.05 (m, 2 H, CHN + CHO), 5.50 (d, ³*J*_{H,H} = 1.8 Hz, 1 H, CHN), 5.67 (d, ³*J*_{H,H} = 2.1 Hz, 1 H, CHN) ppm.

Boc-(L-Oxd)₄-OH (10): Yield: 93% (0.93 mmol, 0.58 g); m.p. 136 °C. $[\alpha]_D^{20}$ = –183.7 (*c* = 1.0, CH₂Cl₂). ¹H NMR (400 MHz, CDCl₃): δ = 1.46 (s, 9 H, *t*Bu), 1.54 (d, ³*J*_{H,H} = 6.0 Hz, 3 H, Me), 1.56 (d, ³*J*_{H,H} = 6.0 Hz, 3 H, Me), 1.60 (d, ³*J*_{H,H} = 5.7 Hz, 3 H, Me), 1.62 (d, ³*J*_{H,H} = 5.7 Hz, 3 H, Me), 4.46 (d, ³*J*_{H,H} = 3.0 Hz, 1 H, CHN), 4.62 (dq, ³*J*_{H,H} = 2.1, 6.0 Hz, 1 H, CHO), 4.78 (dq, ³*J*_{H,H} = 3.0, 6.0 Hz, 1 H, CHO), 4.85–4.98 (m, 2 H, 2 CHN), 5.45 (d, ³*J*_{H,H} = 2.1 Hz, 1 H, CHN), 5.61 (d, ³*J*_{H,H} = 2.1 Hz, 2 H, CHN) ppm. ¹³C NMR (100 MHz, CDCl₃): δ = 20.5, 21.2, 27.7, 61.1, 61.2, 61.7, 61.8, 72.7, 75.3, 75.9, 76.0, 84.5, 148.9, 151.0, 152.2, 152.4, 166.7, 167.0, 168.3, 170.6 ppm. IR (Nujol): $\tilde{\nu}$ = 1790, 1718, 1700 cm^{–1} (C=O). C₂₅H₃₀N₄O₁₅ (626.17): calcd. C 47.93, H 4.83, N 8.94; found C 47.89, H 4.78, N 8.97.

Boc-(L-Oxd)₄-OPfp (11): Yield: 91% (0.91 g, 0.72 g). ¹H NMR (300 MHz, CDCl₃): δ = 1.49 (s, 9 H, *t*Bu), 1.59 (d, ³*J*_{H,H} = 6.3 Hz, 3 H, Me), 1.68 (d, ³*J*_{H,H} = 6.0 Hz, 3 H, Me), 1.70 (d, ³*J*_{H,H} = 5.7 Hz, 3 H, Me), 1.74 (d, ³*J*_{H,H} = 6.0 Hz, 3 H, Me), 4.65 (dq,

$^3J_{\text{H,H}} = 3.0, 6.0 \text{ Hz}$, 1 H, CHO), 4.77 (dq, $^3J_{\text{H,H}} = 2.1, 6.0 \text{ Hz}$, 1 H, CHO), 4.86–4.98 (m, 3 H, CHN + 2 CHO), 5.47 (d, $^3J_{\text{H,H}} = 2.1 \text{ Hz}$, 1 H, CHN), 5.60 (d, $^3J_{\text{H,H}} = 2.1 \text{ Hz}$, 1 H, CHN), 5.62 (d, $^3J_{\text{H,H}} = 1.8 \text{ Hz}$, 1 H, CHN) ppm.

Boc-(L-Oxd)₅-OBn (12): Yield: 50% (0.50 mmol, 0.42 g); m.p. 128–131 °C. $[\alpha]_{\text{D}}^{20} = -215.8$ ($c = 1.0$, CH_2Cl_2). ^1H NMR (400 MHz, CDCl_3): $\delta = 1.52$ (s, 9 H, *t*Bu), 1.59 (d, $^3J_{\text{H,H}} = 6.6 \text{ Hz}$, 3 H, Me), 1.60 (d, $^3J_{\text{H,H}} = 6.3 \text{ Hz}$, 3 H, Me), 1.64 (d, $^3J_{\text{H,H}} = 6.9 \text{ Hz}$, 3 H, Me), 1.66 (d, $^3J_{\text{H,H}} = 6.6 \text{ Hz}$, 3 H, Me), 1.70 (d, $^3J_{\text{H,H}} = 6.3 \text{ Hz}$, 3 H, Me), 4.55 (d, $^3J_{\text{H,H}} = 3.6 \text{ Hz}$, 3 H, CHN), 4.62–4.74 (m, 3 H, 3 CHO), 4.85 (dq, $^3J_{\text{H,H}} = 1.8, 6.6 \text{ Hz}$, CHO), 4.90 (dq, $^3J_{\text{H,H}} = 1.8, 6.3 \text{ Hz}$, CHO), 5.14 (d, $^2J_{\text{H,H}} = 12.0 \text{ Hz}$, 1 H, OCHHPh), 5.27 (d, $^2J_{\text{H,H}} = 12.0 \text{ Hz}$, 1 H, OCHHPh), 5.48 (d, $^3J_{\text{H,H}} = 1.8 \text{ Hz}$, 1 H, CHN), 5.59 (d, $^3J_{\text{H,H}} = 1.5 \text{ Hz}$, 2 H, 2 CHN), 5.63 (d, $^3J_{\text{H,H}} = 1.8 \text{ Hz}$, 1 H, CHN), 7.24–7.48 (m, 5 H, Ph) ppm. ^{13}C NMR (400 MHz, CDCl_3): $\delta = 20.6, 21.0, 21.2, 27.8, 60.9, 61.0, 61.1, 61.2, 61.9, 68.7, 72.7, 75.2, 75.3, 75.7, 75.9, 84.5128.3, 128.5, 128.7, 133.8, 150.8, 151.7, 152.0, 152.2, 152.3, 166.16, 166.8, 167.1, 168.4$ ppm. IR (Nujol): $\tilde{\nu} = 1832, 1792, 1706 \text{ cm}^{-1}$ (C=O). $\text{C}_{37}\text{H}_{41}\text{N}_5\text{O}_{18}$ (843.74): calcd. C 52.67, H 4.90, N 8.30; found C 52.69, H 4.98, N 8.27.

Boc-(L-Oxd)₅-OH (13): Yield: 91% (0.91 mmol, 0.69 g); m.p. 129–132 °C. $[\alpha]_{\text{D}}^{20} = -190.9$ ($c = 0.7$, CH_2Cl_2). ^1H NMR (400 MHz, CDCl_3): $\delta = 1.52$ (s, 9 H, *t*Bu), 1.58–1.75 (m, 15 H, 5 Me), 4.56 (d, $^3J_{\text{H,H}} = 3.6 \text{ Hz}$, 3 H, CHN), 4.69 (dq, $^3J_{\text{H,H}} = 1.9, 6.3 \text{ Hz}$, CHO), 4.78–4.98 (m, 4 H, 4 CHO), 5.50 (d, $^3J_{\text{H,H}} = 2.1 \text{ Hz}$, 1 H, CHN), 5.61 (d, $^3J_{\text{H,H}} = 1.8 \text{ Hz}$, 1 H, CHN), 5.64 (d, $^3J_{\text{H,H}} = 1.5 \text{ Hz}$, 2 H, 2 CHN) ppm. ^{13}C NMR (100 MHz, CDCl_3): $\delta = 20.6, 21.3, 27.9, 60.8, 61.2, 61.3, 62.0, 73.0, 75.4, 75.9, 76.0, 84.8, 149.1, 151.2, 151.9, 152.1, 152.3, 152.4, 166.7, 167.1, 168.4, 169.0$ ppm. IR (Nujol): $\tilde{\nu} = 1792, 1719, 1701 \text{ cm}^{-1}$ (C=O). $\text{C}_{10}\text{H}_{15}\text{NO}_5$ (233.24): calcd. C 47.81, 4.68, N 9.29; found C 47.76, H 4.72, N 9.35.

Computational Methods. All calculations were carried out using the tools available in the Gaussian 98^[29] package on an SGI Origin 3800 multiprocessor system, using the DFT/B3LYP functional (i.e. Becke's three-parameter hybrid functional with the Lee–Yang–Parr correlation functional).^[30] This functional has been shown to properly describe both standard hydrogen bonds,^[31] as well as nonclassical, weakly bound hydrogen bonds (such as C–H...O=C interactions).^[32] In particular, according to the literature,^[33] a mixed basis set was used for the determination of the weak C–H...O=C hydrogen bonds: a 6-31+G(d) basis set for the C*i*A, H*i*A, O(*i*+1)D, C(*i*+1)D atoms (*i* = 1 for dimer; *i* = 1, 2 for trimer; *i* = 1, 2, 3 for tetramer; and *i* = 1, 2, 3, 4 for pentamer) and a 6-31G(d) for all other atoms. Since the O(*i*+1)D lone pairs strongly interact with H*i*A, the use of diffuse functions on heavy atoms is fundamental. Chemical shift simulations were performed by using the standard tools available in the Gaussian 98 package.^[17] A standard 6-31G(d) basis set was used for all the atoms. The computed data do not directly yield the chemical shift value, but only a value for the isotropic magnetic tensor. The chemical shift value is obtained from the equation $\delta_{\text{H}} = 32.18 - \sigma_{\text{H}}$, where 32.18 is the calculated isotropic magnetic tensor for the protons in tetramethylsilane, and σ_{H} is the calculated isotropic magnetic tensor for the investigated proton. This procedure has been recently validated and applied by us for a similar molecular system.^[15]

FT-IR: The FT-IR absorption spectra were recorded with a Perkin–Elmer 1720X spectrophotometer, nitrogen-flushed, equipped with a sample-shuttle device, at 2 cm^{-1} nominal resolution, averaging 100 scans. Solvent (base-line) spectra were recorded

under the same conditions. Cells with path lengths of 0.1, 1.0 and 10 mm (with CaF_2 windows) were used. Spectrograde CDCl_3 (99.8% D) was purchased from Fluka.

^1H NMR: The ^1H NMR spectra were recorded with a Bruker AM 400 spectrometer. Measurements were carried in deuteriochloroform (99.96% D; Aldrich) and dimethyl sulfoxide ($[\text{D}_6]\text{DMSO}$) (99.96% D₆; Acros Organics) with tetramethylsilane as the internal standard.

CD: The CD spectra were obtained with a Jasco J-710 spectropolarimeter. Cylindrical fused quartz cells of 10, 1, 0.2 and 0.1 mm path length (Hellma) were used. The values are expressed in terms of $[\theta]_{\text{T}}$, the total molar ellipticity ($\text{deg} \times \text{cm}^2 \times \text{dmol}^{-1}$). Spectrograde MeOH (Baker) was used as solvent.

Acknowledgments

M. G., F. B., S. L., C. T., and V. T. thank MURST (Cofin 2000, Cofin 2001 and 60%), the Alma Mater Studiorum – University of Bologna (Funds for Selected Topics) and CINECA (Grant K11-BOZZ1) for financial support.

- [1] S. H. Gellman, *Acc. Chem. Res.* **1998**, *31*, 173–180.
- [2] C. Tomasini, A. Vecchione, *Org. Lett.* **1999**, *1*, 2153–2156.
- [3] G. Valle, C. Toniolo, G. Jung, *Liebigs Ann. Chem.* **1986**, 1809–1822.
- [4] S. Lucarini, C. Tomasini, *J. Org. Chem.* **2001**, *66*, 727–732.
- [5] A. J. Hopfinger, in *Conformational Properties of Macromolecules*, Academic Press, New York, **1973**, pp. 182–189, and references therein.
- [6] [6a] S. M. Newman, A. Kutner, *J. Am. Chem. Soc.* **1951**, *73*, 4199–4204. [6b] J. B. Hyne, *J. Am. Chem. Soc.* **1959**, *81*, 6058–6061. [6c] W. D. Lubell, H. Rapoport, *J. Org. Chem.* **1989**, *54*, 3824–3831.
- [7] D. J. Ager, I. Prakash, D. R. Schaad, *Chem. Rev.* **1996**, *96*, 835–875.
- [8] [8a] D. A. Evans, J. Bartroli, T. L. Shih, *J. Am. Chem. Soc.* **1981**, *103*, 2127–2129. [8b] D. A. Evans, M. D. Ennis, D. J. Mathre, *J. Am. Chem. Soc.* **1982**, *104*, 1737–1739. [8c] D. A. Evans, J. V. Nelson, T. R. Taber, *Top. Stereochem.* **1982**, *13*, 1–115.
- [9] [9a] D. A. Evans, J. M. Takacs, L. R. McGee, M. D. Ennis, D. J. Mathre, J. Bartroli, *Pure Appl. Chem.* **1981**, *53*, 1109–1127. [9b] D. A. Evans, *Aldrichim. Acta* **1982**, *15*, 23–32. [9c] D. A. Evans, D. L. Rieger, M. T. Bilodeau, F. Urpi, *J. Am. Chem. Soc.* **1991**, *113*, 1047–1049.
- [10] [10a] D. A. Evans, K. T. Chapman, J. Bisaha, *J. Am. Chem. Soc.* **1984**, *106*, 4261–4263. [10b] D. A. Evans, K. T. Chapman, J. Bisaha, *J. Am. Chem. Soc.* **1988**, *110*, 1238–1256. [10c] D. A. Evans, K. T. Chapman, D. T. Hung, A. T. Kawaguchi, *Angew. Chem. Int. Ed. Engl.* **1987**, *26*, 1184–1186.
- [11] E. Falb, A. Nudelman, A. Hassner, *Synth. Commun.* **1993**, *23*, 2839–2844.
- [12] [12a] S. S. Canan Koch, A. R. Chamberlin, *J. Org. Chem.* **1993**, *58*, 2725–2737. [12b] J. R. Gage, D. A. Evans, *Org. Synth.* **1990**, *68*, 83–91.
- [13] G.-J. Ho, D. J. Mathre, *J. Org. Chem.* **1995**, *60*, 2271–2273.
- [14] M. Green, M. Berman, *Tetrahedron Lett.* **1990**, *31*, 5851–5854.
- [15] F. Bernardi, M. Garavelli, M. Scatizzi, C. Tomasini, V. Trigari, M. Crisma, F. Formaggio, C. Peggion, C. Toniolo, *Chem. Eur. J.* **2002**, *8*, 2516–2525.
- [16] [16a] F. H. Allen, O. Kennard, R. Taylor, *Acc. Chem. Res.* **1983**, *16*, 146–153. [16b] P. Chakrabarti, S. Chakrabarti, *J. Mol. Biol.* **1998**, *284*, 867–873. [16c] G. Felcy Fabiola, S. Krishnaswamy, V. Nagarajan, V. Pattabhi, *Acta Crystallogr.* **1997**, *D53*, 316–320. [16d] J. Bella, H. M. Berman, *J. Mol. Biol.* **1996**, *264*, 734–742. [16e] Z. S. Derewenda, L. Lee, V. Derewenda, *J. Mol.*

- Biol.* **1995**, 252, 248–262. ^[16f] T. Steiner, *J. Chem. Soc., Perkin Trans. 2* **1995**, 1315–1319. ^[16g] G. R. Desiraju, *Acc. Chem. Res.* **1996**, 29, 441–449. ^[16h] T. Steiner, W. Saenger, *J. Am. Chem. Soc.* **1992**, 114, 10146–10154. ^[16i] G. R. Desiraju, *The Weak Hydrogen Bond in Structural Chemistry and Biology*, Oxford Science, Oxford, U. K., **1999**.
- ^[17] ^[17a] K. Wolinski, J. F. Hilton, P. Pulay, *J. Am. Chem. Soc.* **1990**, 112, 8251–8260. ^[17b] K. Wolinski, A. J. Sadlej, *Mol. Phys.* **1980**, 41, 1419–1430. ^[17c] R. Ditchfield, *Mol. Phys.* **1974**, 27, 789–807. ^[17d] R. McWeeny, *Phys. Rev.* **1962**, 126, 1028–1024. ^[17e] F. London, *J. Phys. Radium* **1937**, 8, 397–409.
- ^[18] A. Bagno, *Chem. Eur. J.* **2001**, 7, 1652–1660.
- ^[19] ^[19a] L. J. Bellamy, in *The Infrared Spectra of Complex Molecules*, Methuen, London, **1966**. ^[19b] W. L. Driessen, P. L. A. Everstijn, *J. Coord. Chem.* **1980**, 10, 155–158.
- ^[20] A. Bavoso, E. Benedetti, B. Di Blasio, V. Pavone, C. Pedone, C. Toniolo, G. M. Bonora, *Macromolecules* **1982**, 15, 54–59.
- ^[21] ^[21a] K. D. Kopple, M. Ohnishi, A. Go, *Biochemistry* **1969**, 8, 4087–4095. ^[21b] D. Martin, G. Hauthal, in *Dimethyl Sulfoxide*, Van Nostrand-Reinhold, Wokingham, U. K., **1975**.
- ^[22] D. S. Wishart, B. D. Sykes, F. M. Richards, *J. Mol. Biol.* **1991**, 222, 311–333.
- ^[23] Y. Xu, P. Saweczko, H.-B. Kraatz, *J. Organomet. Chem.* **2001**, 637–639, 335–342.
- ^[24] T. Polonski, *J. Chem. Soc., Perkin Trans. 1* **1988**, 629–637.
- ^[25] D. J. Hill, M. J. Mio, R. B. Prince, T. S. Hughes, J. S. Moore, *Chem. Rev.* **2001**, 101, 3893–4011.
- ^[26] E. Benedetti, A. Bavoso, B. Di Blasio, V. Pavone, C. Pedone, C. Toniolo, G. M. Bonora, *Biopolymers* **1983**, 22, 305–317.
- ^[27] L. Halab, F. Gosselin, W. D. Lubell, *Biopolymers (Pept. Sci.)* **2000**, 55, 101–122.
- ^[28] L. Halab, W. D. Lubell, *J. Pept. Sci.* **2001**, 7, 92–104.
- ^[29] M. J. Frisch, G. W. Trucks, H. B. Schlegel, G. E. Scuseria, M. A. Robb, J. R. Cheeseman, V. G. Zakrzewski, J. A. Montgomery Jr., R. E. Stratmann, J. C. Burant, S. Dapprich, J. M. Millan, A. D. Daniels, K. N. Kudin, M. C. Strain, O. Farkas, J. Tomasi, V. Barone, M. Cossi, R. Cammi, B. Mennucci, C. Pomelli, C. Adamo, S. Clifford, J. Ochterski, G. A. Patersson, P. Y. Ayala, Q. Cui, K. Morokuma, D. K. Malik, A. D. Rabuck, K. Raghavachari, J. B. Foresman, J. Cioslowski, J. V. Ortiz, A. G. Baboul, B. B. Stefanov, G. Liu, A. Liashenko, P. Piskorz, I. Komaromi, R. Gomperts, R. L. Martin, D. J. Fox, T. Keith, M. A. Al-Laham, C. Y. Peng, A. Nanayakkara, M. Challacombe, P. M. W. Gill, B. Johnson, W. Chen, M. W. Wong, J. L. Andres, C. Gonzales, M. Head-Gordon, E. S. Replogle, J. Pople, *Gaussian 98, Revision A.9*, Gaussian Inc., Pittsburgh, PA, **1998**.
- ^[30] A. D. Becke, *J. Chem. Phys.* **1993**, 98, 5648–5652.
- ^[31] ^[31a] L. Gonzalez, O. Mo, M. Yanez, *J. Comput. Chem.* **1997**, 18, 1124–1135. ^[31b] R. A. Klein, *J. Comput. Chem.* **2002**, 23, 585–599. ^[31c] J. J. Novoa, C. Sosa, *J. Phys. Chem.* **1995**, 99, 15837–15845.
- ^[32] L. Brunel, F. Carre', S. G. Dutremez, C. Guerin, F. Dahan, O. Eisenstein, G. Sini, *Organometallics* **2001**, 20, 47–54.
- ^[33] J. J. Novoa, B. Tarron, M.-H. Whangbo, J. M. Williams, *J. Chem. Phys.* **1991**, 95, 5179–5186.

Received June 7, 2002

[O02309]